International Journal of Thermophysics, Vol. 21, No. 2, 2000

Thermodynamic Properties of Trifluoroiodomethane (CF_3I)[1]

Y. Y. Duan,[2] L. Shi,[2] L. Q. Sun,[2] M. S. Zhu,[2,3] and L. Z. Han[2]

Studies of the thermodynamic properties of trifluoroiodomethane (CF_3I) are presented in this paper. The vapor–liquid coexistence curve of CF_3I was measured by visual observation of the meniscus. The critical temperature and the critical density of CF_3I were determined by considering not only the level where the meniscus disappeared but also the intensity of the critical opalescence. The correlation of the saturated density in the critical region was developed, and the exponent of the power law β was determined. Correlations of the saturated vapor and liquid densities and the enthalpy of vaporization for CF_3I were also developed. The vapor pressure of CF_3I was measured at temperatures ranging from below the normal boiling point to the critical point, and a vapor pressure equation for CF_3I was developed, from which the normal boiling point of CF_3I was determined. The gaseous PVT properties of CF_3I were measured with a Burnett/isochoric method, and a gaseous equation of state for CF_3I was developed. The speed of sound of gaseous CF_3I was measured with a cylindrical, variable-path acoustic interferometer operating at 156.252 kHz, and the ideal-gas heat capacity and second acoustic virial coefficient were calculated. A correlation of the second virial coefficient for CF_3I was obtained by a semiempirical method using the square-well potential for the intermolecular force and was compared with the result based on PVT measurements. The surface tension of CF_3I was measured with a differential capillary rise method (DCRM), and the temperature dependence of the results was successfully represented to within $\pm 0.13\ \mathrm{mN \cdot m^{-1}}$ using a van der Waals correlation.

KEY WORDS: critical parameters; equation of state; ideal-gas heat capacity; PVT; speed of sound; surface tension; trifluoroiodomethane; vapor pressure.

[1] Paper presented at the Fifth Asian Thermophysical Properties Conference, August 30–September 2, 1998, Seoul, Korea.

[2] Department of Thermal Engineering, Tsinghua University, Beijing 100084, People's Republic of China.

[3] To whom correspondence should be addressed.

0195-928X/00/0300-0393$18.00/0

1. INTRODUCTION

As a traditional and effective refrigerant, CFC-12 has been widely used in numerous applications. Revisions to the Montreal Protocol have set the phase-out dates for CFCs with significant ozone depletion potential and global warming potential. HFC-134a has been widely used as a replacement for CFC-12, especially in the United States, Japan, the United Kingdom, and France. HFC-134a, however, usually requires a retrofit of existing equipment and is immiscible with conventional lubricants. It also has a relatively high global warming potential (GWP). Even though they are flammable, hydrocarbons are also considered to be promising alternatives, especially in Germany. CF_3I has been found to be non-ozone depleting (ODP = 0), miscible with mineral oil, and compatible with materials of refrigeration systems. It also has an extremely low GWP value (<50). Therefore, it is also being considered as a promising alternative, especially as a component in mixtures, to replace CFC-12 [1, 2]. Unfortunately, reliable thermophysical property data for CF_3I are limited.

In 1995 we began a systematic and comprehensive research program on the thermophysical properties of CF_3I. In this paper, we report results for the thermodynamic properties of CF_3I which include critical parameters, saturated vapor and liquid densities, vapor pressures, PVT, speed of sound, surface tension, etc.

The CF_3I sample was provided by IKON Co. and was used without further purification. The manufacturer stated that the sample purity of CF_3I was 99.95 wt. % with 3.4 ppm of water.

2. CRITICAL PARAMETERS AND SATURATED DENSITY

The vapor–liquid coexistence curve of trifluoroiodomethane (CF_3I) was measured by visual observation of the meniscus disappearance in an optical cell [3]. Thirty-two data points of saturated densities along the vapor–liquid coexistence curve between 384 and 2024 $kg \cdot m^{-3}$ have been obtained in the temperature range from 301 K to the critical temperature. The experimental uncertainties in temperature and density were estimated to be within ± 10 mK and $\pm 0.5\%$, respectively. On the basis of these measurements near the critical point, a critical temperature of $T_c = 396.44 \pm 0.01$ K and a critical density of $\rho_c = 868 \pm 3\ kg \cdot m^{-3}$ for CF_3I were determined by considering the meniscus disappearance level as well as the intensity of the critical opalescence. The critical pressure of $p_c = 3.953 \pm 0.005$ MPa was determined by extrapolation of the vapor pressure correlation, discussed later, using the present T_c value.

Table I. Critical Parameters of CF_3I

First author	Year	Ref.	T_c (K)	ρ_c (kg · m^{-3})	p_c (MPa)
Sladkov	1991	4	395.15	871	4.04
UNEP	1994	5	395.05	—	4.04
Duan	1996	6	395.05	—	3.862
This work	1998		396.44 ± 0.01	868 ± 3	3.953 ± 0.005

Table I compares the present critical parameters with those determined by other authors. The present ρ_c value is in good agreement with the value of Sladkov and Bogacheva [4], but the present T_c value is higher than that of Sladkov and Bogacheva [4] and UNEP [5] by 1.29 and 1.39 K, respectively, and the present p_c value is lower than those of Sladkov and Bogacheva and UNEP. The p_c value of Duan et al. [6] was determined by extrapolation of vapor pressure measurements using the T_c value of UNEP; it is lower than the present p_c value.

The critical exponent β is important for modeling the vapor–liquid coexistence curve in the critical region by means of the following power-law representation:

$$(\rho' - \rho'')/2\rho_c = B[(T_c - T)/T_c]^{\beta} \tag{1}$$

where ρ', ρ'', T, ρ_c, T_c, and B denote the saturated liquid density, the saturated vapor density, the temperature, the critical density, the critical temperature, and the critical amplitude, respectively. The correlation of the vapor–liquid coexistence curve was formulated by using the Wagner expansion [7]:

$$\Delta\rho^* = D_0 |\Delta T^*|^{(1-\alpha)} + D_1 |\Delta T^*| + D_2 |\Delta T^*|^{(1-\alpha+\Delta_1)} \pm B_0 |\Delta T^*|^{\beta} \pm B_1 |\Delta T^*|^{(\beta+\Delta_1)} \tag{2}$$

where $\Delta\rho^* = (\rho - \rho_c)/\rho_c$ and $\Delta T^* = (T - T_c)/T_c$. The exponents are $\alpha = 0.1085$, $\beta = 0.325$, and $\Delta_1 = 0.50$. The coefficients $D_0 = -12.61779$, $D_1 = 21.11048$, $D_2 = -10.43621$, $B_1 = 1.572056$, and $B_2 = 0.7606325$ were determined by fitting Eq. (2) to the experimental data over the reduced temperature range $T/T_c > 0.93$. The upper (+) and lower signs (−) of the fourth and fifth terms in Eq. (2) correspond to the saturated liquid and vapor, respectively. The saturation curves calculated from Eq. (2) are shown in Fig. 1. Figure 2 shows logarithmic plots in terms of the experimental data and calculated results from Eq. (2). Fifteen measured data points near the critical point were used for the determination of the

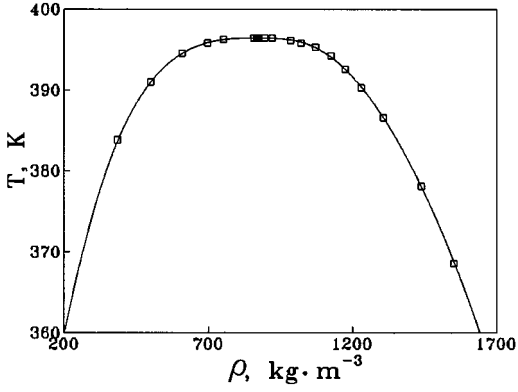

Fig. 1. Vapor–liquid coexistence in the critical region of CF_3I. (□) Experimental data; (■) critical point.

critical exponent β and the critical amplitude B for the least-squares fit. These values are $\beta = 0.342$ and $B = 1.810$.

There are only three saturated density data points available in the literature [8, 9]. Based on the new experimental data and extrapolating saturated vapor densities from PVT measurement of CF_3I, correlations of saturated liquid and vapor densities were developed as [3]

$$\rho_r = 1 + b_1\tau^{\beta} + b_2\tau^{2\beta} + b_3\tau + b_4\tau^{1/\beta} \tag{3}$$

where $\rho_r = \rho/\rho_c$, $\rho_c = 868\ \mathrm{kg \cdot m^{-3}}$ is the critical density, $\beta = 0.325$ is the critical exponent, and b_1, b_2, b_3, b_4 are coefficients determined by fitting

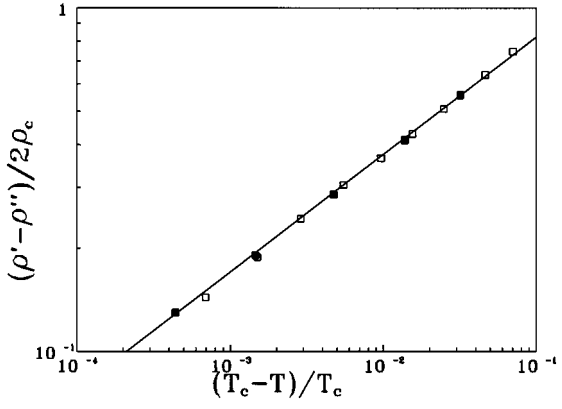

Fig. 2. Critical exponent and amplitude of CF_3I. (□) Saturated liquid; (■) Saturated vapor.

Table II. Coefficients of Eq. (3)

	b_1	b_2	b_3	b_4
Saturated liquid	1.401532	0.8092603	0.5946375	−0.3991380
Saturated vapor	−1.542282	−1.149425	2.020176	−0.3776717

Eq. (3) to the data. The coefficients of Eq. (3) for the saturated liquid and vapor are given in Table II.

The relative deviations of the experimental data and calculated results from Eq. (3) are shown in Fig. 3; the maximum deviation is less than 1%. Equation (3) is valid at temperatures from 195 K to the critical point for the saturated liquid and from 233 K to the critical point for the saturated vapor.

3. VAPOR PRESSURE AND ENTHALPY OF VAPORIZATION

Sixty-four vapor pressure data points for CF_3I were measured for the temperature range from 243 to 393 K [6], as shown in Fig. 4. The uncertainties of temperatures and pressures were ±10 mK and ±500 Pa, respectively. Based on the experimental results and using the new experimental

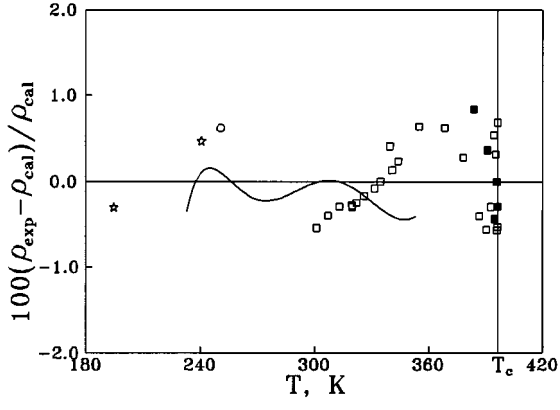

Fig. 3. Relative deviations of experimental saturated densities from Eq. (3). (□) Present saturated liquid density; (■) present saturated vapor density; (○) Emeleus and Wood [8] (liquid); (☆) Nodiff et al. [9] (liquid); (——) saturated vapor density calculated from Eq. (7).

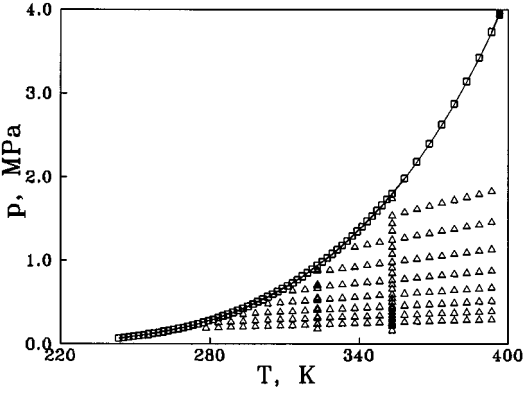

Fig. 4. Experimental vapor pressure and PVT data for CF_3I. (■) Critical point; (□) vapor pressure; (——) vapor pressure equation; (△) PVT.

critical parameters of the present work, a new Wagner-type vapor pressure equation for CF_3I was developed as follows:

$$\ln p_r = (A_1\tau + A_2\tau^{1.25} + A_3\tau^3 + A_4\tau^7)\, T_c/T \tag{4}$$

where $p_r = p/p_c$, $p_c = 3.953$ MPa is the critical pressure, which is an adjustable parameter in the correlation, $\tau = 1 - T/T_c$, and $T_c = 396.44$ K is the critical temperature. The coefficients $A_1 = -7.204825$, $A_2 = 1.393833$, $A_3 = -1.568372$, and $A_4 = -5.776895$ were determined by fitting Eq. (4) to the data. Equation (4) is valid at temperatures from 243 K to the critical point. The normal boiling point was also determined, $T_b = 251.315 \pm 0.010$ K. Available normal boiling point data are listed in Table III.

Figure 5 shows the pressure deviations of the experimental data from Eq. (4); the maximum deviation is 0.11% and the RMS deviation is 0.035%. Most of the absolute deviations are less than ± 500 Pa.

Table III. Normal Boiling Point Data for CF_3I

First author	Year	Ref.	Normal boiling point T_b
Haszeldine	1952	10	−22°C
Nodiff	1953	9	−22.5°C
Iarovenko	1958	11	−22.5°C
Zwolinski	1976	12	−22 ± 1°C
Present work	1998		251.315 ± 0.010 K

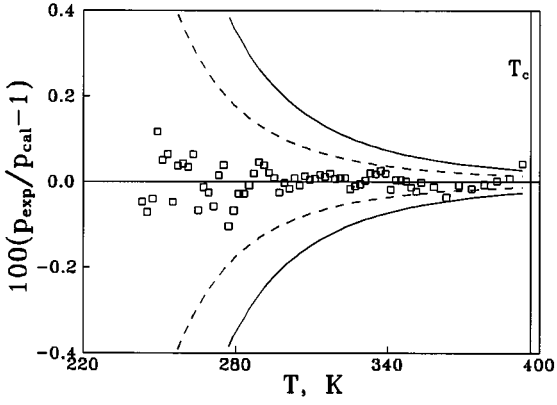

Fig. 5. Deviations of experimental vapor pressure data from vapor pressure equation for CF_3I. (– –) ± 500 Pa; (——) ± 1 kPa.

According to the Clapeyron equation, the enthalpy of vaporization can be determined from

$$r = h'' - h' = \left(\frac{dp}{dT}\right)_\sigma T\left(\frac{1}{\rho''} - \frac{1}{\rho'}\right) \tag{5}$$

where r is the enthalpy of vaporization, $(dp/dT)_\sigma$ is the first derivative of the vapor pressure, h'' and h' are the enthalpies of the saturated vapor and liquid, respectively, and ρ'' and ρ' are the densities of the saturated vapor and liquid, respectively. $(dp/dT)_\sigma$ is calculated from Eq. (4), and ρ'' and ρ' are calculated from Eq. (3).

The enthalpy of vaporization of CF_3I was calculated from Eq. (5) and correlated by the following equation:

$$r/RT_c = b_0\tau^\beta + b_1\tau^{\beta+\Delta_1} + b_2\tau^{1-\alpha+\beta} + \sum_{i=1}^{3} a_i\tau^i \tag{6}$$

where $\tau = 1 - T/T_c$, $\alpha = 0.1085$, and $\beta = 0.325$ are the critical exponents, and $\Delta_1 = 0.50$ is the first symmetric correlation-to-scaling exponent. The coefficients $b_0 = 5.803533$, $b_1 = 10.82942$, $b_2 = -3.123554$, $a_1 = -2.561332$, $a_2 = -10.58599$, and $a_3 = 8.230100$ were determined by fitting Eq. (6) to the data calculated from Eq. (5). Equation (6) is valid from 233 K to the critical point, and the uncertainty of Eq. (6) is estimated to be within $\pm 2\%$.

4. PVT PROPERTIES

One hundred and seventy-five PVT data points for gaseous CF_3I were measured by Burnett/isochoric method and are shown in Fig. 4. The results ranged from 278 to 393 K in temperature, 0.19 to 1.75 MPa in pressure, and 12 to 163 $kg \cdot m^{-3}$ in density, respectively. The uncertainties of the measurements for temperatures and pressures were ± 10 mK and ± 500 Pa, respectively [13].

The experimental data were represented with a three-term virial equation:

$$\frac{P}{\rho RT} = 1 + B\rho + C\rho^2 + D\rho^3$$

$$\begin{aligned} B &= B_0 + B_1 T_r^{-1} + B_2 T_r^{-2} + B_3 T_r^{-3} + B_4 T_r^{-6} + B_5 T_r^{-8} \\ C &= C_0 T_r^{-5} + C_1 T_r^{-6} \\ D &= D_0 + D_1 T_r \end{aligned} \tag{7}$$

where $T_c = 396.44$ K is the critical temperature, $T_r = T/T_c$, and $R = 42.4402\ J \cdot K^{-1} \cdot kg^{-1}$. The coefficients $B_0 = 0.1017782$, $B_1 = -0.3547075$, $B_2 = 0.4369783$, $B_3 = -0.1979620$, $B_4 = 0.01492476$, $B_5 = -2.31700 \times 10^{-3}$, $C_0 = -1.14023 \times 10^{-6}$, $C_1 = 9.84870 \times 10^{-7}$, $D_0 = 8.98114 \times 10^{-9}$, and $D_1 = -8.64263 \times 10^{-9}$ were determined by fitting Eq. (7) to the experimental data. The pressure and density deviations of the experimental data from Eq. (7) are shown in Figs. 6 and 7, respectively. The maximum and RMS deviations are 0.41% and 0.11% for pressure and 0.49% and 0.12% for density, respectively.

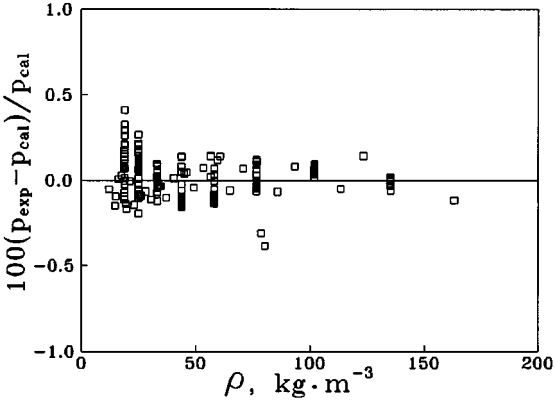

Fig. 6. Pressure deviations of experimental PVT data from equation of state for CF_3I.

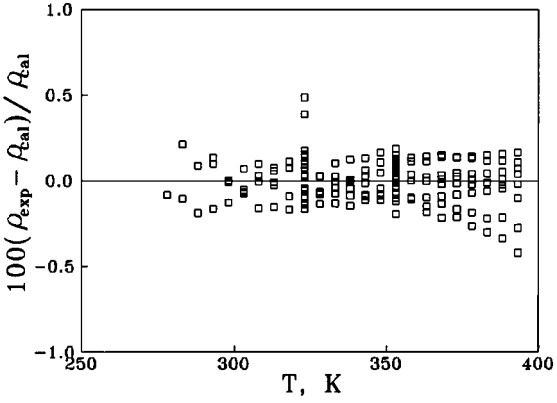

Fig. 7. Density deviations of experimental PVT data from equation of state for CF_3I.

5. SPEED OF SOUND

According to speed-of-sound data, the ideal-gas heat capacity at constant pressure and the virial coefficient can be derived. There are no reliable speed-of-sound data published before this study, and only one set of ideal-gas heat capacity data at constant pressure in the temperature range from 0 to 1500 K was reported by Kudchadker and Kudchadker [14]. The speed of sound of gaseous CF_3I was measured at temperatures from 273 to 333 K and pressures from 58 to 276 kPa with a cylindrical, variable-path acoustic interferometer operating at 156.252 kHz. The speed-of-sound results of CF_3I were obtained from the corrected wavelengths together with the fixed frequency. Figure 8 shows the measured speed-of-sound results

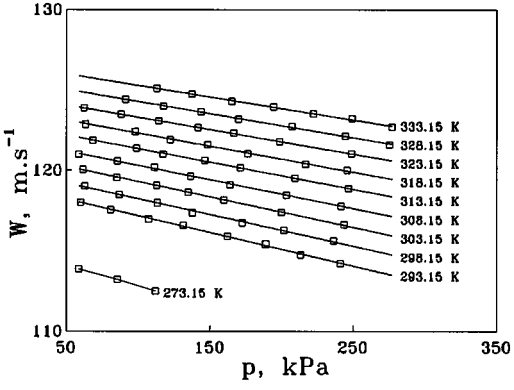

Fig. 8. Speed-of-sound data for gaseous CF_3I.

versus pressure along each isotherm. The uncertainty of the speed-of-sound measurements was less than $\pm 0.1\%$ [15].

According to thermodynamic relations, the ideal-gas heat capacity at constant pressure C_p^0 and the second acoustic virial coefficient β_a can be determined using the speed-of-sound results; the C_p^0 and β_a data were correlated by the following equations:

$$C_p^0/R = -1.87904 + 0.0550142T - 7.2558 \times 10^{-5} T^2 \quad (8)$$

$$\beta_a\,(\mathrm{cm^3 \cdot mol^{-1}}) = -7.24777 \times 10^3 + 36.4017T - 0.0450024T^2 \quad (9)$$

The maximum deviation of the measured ideal-gas heat capacity data from Eq. (8) was less than 0.5%. The results of Kudchadker and Kudchadker [14] are higher than calculated values from Eq. (8) by about 6% to 7%. The maximum deviation of the second acoustic virial coefficient data from Eq. (9) is less than 1.1%.

Based on the measurements, the second virial coefficient B of CF_3I was obtained by a semiempirical method using the square-well potential for the intermolecular force, and it was correlated as

$$B\,(\mathrm{cm^3 \cdot mol^{-1}}) = 82.65\{1 - 1.173[\exp(605/T) - 1]\} \quad (10)$$

Figure 9 shows the second virial coefficient B versus the temperature for a temperature range from 270 to 390 K calculated with Eq. (10) and derived from PVT measurements.

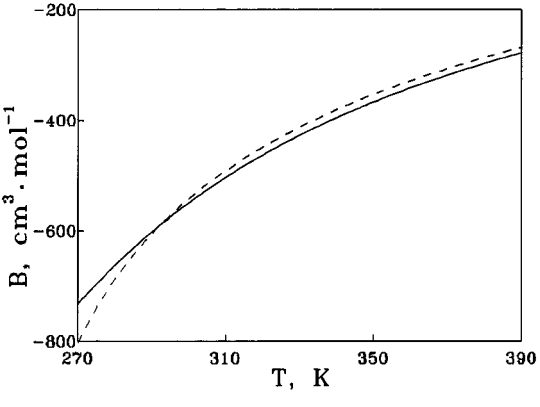

Fig. 9. Second virial coefficient versus temperature for CF_3I. (– –) Derived from Eq. (7); (——) Eq. (10).

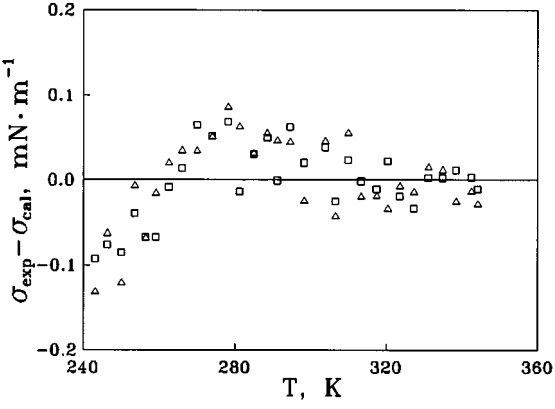

Fig. 10. Absolute deviations of experimental surface tension results from Eq. (11). (□) Capillaries 1 and 2; (△) capillaries 1 and 3.

6. SURFACE TENSION

Surface tension data for CF_3I have been measured with a differential capillary rise method (DCRM). The sample cell of the measurement system contained three capillaries with the following bore radii: $r_1 = 0.127 \pm 0.001$ mm, $r_2 = 0.259 \pm 0.001$ mm, and $r_3 = 0.390 \pm 0.001$ mm. Measurements were conducted under equilibrium conditions between the liquid and its saturated vapor. Two data sets for a total of 60 surface tension data points for CF_3I were measured in the temperature range from 243 to 344 K using capillaries 1 and 2 and capillaries 1 and 3 [16]. The saturated liquid and vapor densities of CF_3I were calculated from Eq. (3). A van der Waals-type surface tension correlation was used to correlate the experimental data,

$$\sigma = \sigma_0(1 - T/T_c)^n \tag{11}$$

where σ is the surface tension, $\sigma_0 = 57.306\ \text{mN} \cdot \text{m}^{-1}$, and $n = 1.2933$ as determined by a least-squares fit. Figure 10 shows absolute deviations of the experimental data from Eq. (11); most of the deviations are less than $\pm 0.1\ \text{mN} \cdot \text{m}^{-1}$. Maximum deviations of the experimental data from Eq. (11) are less than 0.8%, and the RMS deviation is 0.58%.

ACKNOWLEDGMENTS

This work was supported by the State Education Commission of China (Grant No. 9400364). We are grateful to Dr. Nimitz, IKON Co., for

providing the CF_3I sample. We also thank Yi-Dong Fu for providing useful help with the measurements.

REFERENCES

1. L. Lankford and J. Nimitz, in *Proc. International CFC and Halon Alternatives Conf.* (Washington, D.C., 1993), p. 141.
2. M. S. Zhu, X. Y. Zhao, L. Shi, and L. Z. Han, *J. Tsinghua Univ.* **37**:81 (1997).
3. Y. Y. Duan, L. Shi, M. S. Zhu, and L. Z. Han, *J. Chem. Eng. Data* **44**:501 (1999).
4. I. B. Sladkov and A. V. Bogacheva, *Zh. Priklad. Khim.* **64**:2435 (1991).
5. UNEP, *1994 Report of the Refrigeration, Air Conditioning and Heat Pumps Technical Options Committee* (Nairobi, UNEP, 1995).
6. Y. Y. Duan, M. S. Zhu, and L. Z. Han, *Fluid Phase Equil.* **121**:227 (1996).
7. J. M. H. Levelt Sengers and J. V. Sengers, in *Perspectives in Statistical Physics*, H. J. Raveche, ed. (North-Holland, Amsterdam, 1981), Chap. 14.
8. H. J. Emeleus and J. F. Wood, *J. Chem. Soc.* 2153 (1948).
9. E. A. Nodiff, A. V. Grosse, and M. Hauptshein, *J. Org. Chem.* 235 (1953).
10. R. N. Haszeldine, *J. Chem. Soc.* 4259 (1952).
11. N. N. Iarovenko, *J. Gen. Chem. USSR* **28**:2543 (1958).
12. B. J. Zwolinski, Thermodynamics Research Center Data Project, Thermodynamics Research Center, Loose-leaf data sheets (Texas A&M University, College Station, Texas, 1976).
13. Y. Y. Duan, M. S. Zhu, and L. Z. Han, *Fluid Phase Equil.* **131**:233 (1997).
14. S. A. Kudchadker and A. P. Kudchadker, *J. Phy. Chem. Ref. Data* **7**:425 (1978).
15. Y. Y. Duan, L. Q. Sun, L. Shi, M. S. Zhu, and L. Z. Han, *Fluid Phase Equil.* **137**:121 (1997).
16. Y. Y. Duan, L. Shi, M. S. Zhu, and L. Z. Han. *Fluid Phase Equil.* **154**:71 (1999).